ACS APPLIED MATERIALS & INTERFACES

Research Article

www.acsami.org

Macroporous Graphene Oxide–Polymer Composite Prepared through Pickering High Internal Phase Emulsions

Zheng Zheng, Xianhua Zheng, Haitao Wang,* and Qiangguo Du

State Key Laboratory of Molecular Engineering of Polymers, Department of Macromolecular Science, Fudan University, Shanghai 200433, P. R. China

Supporting Information

ABSTRACT: Macroporous polymer–graphene oxide (GO) composites were successfully prepared using Pickering high internal phase emulsion (HIPE) templates. GO flakes were modified by the cationic surfactant cetyltrimethylammonium bromide (CTAB) and used as the stabilizer of water-in-oil (W/O) Pickering emulsions. CTAB-modified GO is effective at stabilizing W/O Pickering HIPEs, and the lowest GO content is only about 0.2 mg mL^{-1} (relative to the volume of the oil phase). The close-cell morphology of the resulting poly-Pickering HIPEs is observed, and the void size of the porous polymers is tuned by varying the concentration of GO. Three-dimensional macroporous chemically modified graphene (CMG) monoliths with a high specific surface area of about 490 m^2 g^{-1} were obtained after removing the cellular polymer substrates through calcination. The micropores were also found in CMGs, which may be caused by the decomposition of CTAB adsorbed on the surface of GO.

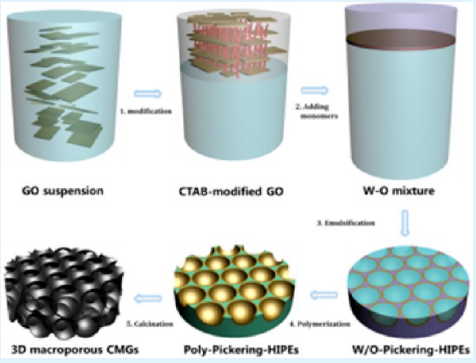

KEYWORDS: *chemically modified graphene, high internal phase emulsions, macroporous polymers, Pickering emulsions, surface modification*

INTRODUCTION

High internal phase emulsions (HIPEs) are usually defined as concentrated emulsions where the volume fraction of the internal phase is larger than 0.74 (the maximum value for compact packing of monodispersed spherical droplets).[1] Macroporous polymers obtained from HIPE templates have gained great interest for many years because of their well-defined structure.[2−4] Recently, particle-stabilized HIPEs, also known as Pickering HIPEs, have been used as templates to prepare highly porous polymers termed poly-Pickering HIPEs. Compared with conventional HIPEs stabilized by molecular surfactants such as poly(oxyethylene) sorbitan monostearate (Tween 80), sorbitan monooleate (Span 80), and poly(oxyethylene) lauryl ether (Brij 30),[2] Pickering HIPEs have a number of advantages. First, solid-particle-stabilized (Pickering) HIPEs are extremely stable resulting from the irreversible adhesion of solid particles at the liquid–liquid interface.[5,6] Therefore, a much smaller amount of solid particles is needed to stabilize HIPEs.[2,3,7] Second, poly-Pickering HIPEs are more favorable for use in biomaterials because solid particles are normally less toxic than surfactants.[8] Third, the mechanical properties of macroporous polymers may be improved when inorganic nanoparticles are used as a Pickering stabilizer.[9] Furthermore, the functional particles used to stabilize emulsions also render poly-Pickering HIPEs with some new features,[10,11] for instance, magnetic macroporous polymers.[11] Thus far, poly-Pickering HIPEs have been successfully prepared using various solid particles such as polymer particles,[12,13] silica,[7,14] titania,[15] iron oxide nanoparticles,[11] and carbon nanotubes.[10,16]

It has been proven that GO can be used as a Pickering stabilizer because of its amphiphilicity.[17,18] Latex particles were synthesized from GO-stabilized oil-in-water (O/W) Pickering emulsion templates.[19,20] By taking advantage of the amphiphilicity of GO nanosheets and the interaction between the polymer and stabilizer, GO-coated PS microspheres have been prepared in our previous work.[21] To the best of our knowledge, macroporous polymers fabricated via GO-stabilized HIPEs have been seldom reported.

It is well known that GO is normally used to produce graphene sheets.[22,23] Graphene has numerous potential applications because of its extraordinary electronic, thermal, and mechanical properties.[24−30] Small graphene sheets are usually needed to form macroscopic constructions for practical applications in the energy, sensing, and biological fields.[31−33] In recent years, the assembly of 2D graphene or chemically modified graphene (CMG) sheets into macroscopic 3D architectures has been studied extensively.[34−38] Three-dimensional graphene (CMG)-based materials with a large surface area and specific morphologies have been prepared via various strategies such as gelation of CMGs,[39] the breath-figure method,[40] unidirectional freezing,[37] tap casting,[41] template-

Received: May 29, 2013
Accepted: July 18, 2013
Published: July 18, 2013

directed chemical vapor deposition (CVD),[38,42] and the sacrificial templates method.[43−45]

Herein, we successfully prepared macroporous polymers via Pickering HIPE templates. The hydrophobicity of GO flakes is greatly improved by the adsorption of CTAB molecules on the surface, and the modified GO is used as the stabilizer to produce the W/O Pickering HIPEs. The void size of the macroporous polymers depends on the GO concentration. Three-dimensional macroporous CMG monoliths with a high specific surface area of about 490 m^2 g^{-1} are also fabricated using porous polymers as the sacrificial templates. The microporous structure in CMGs may be ascribed to the decomposition of CTAB adsorbed on the surface of GO.

EXPERIMENTAL SECTION

Materials. Sulfuric acid (98%), potassium permanganate (99%), sodium nitrate (99%), hydrogen peroxide (30%), hydrochloric acid (37%), styrene (99%), azo-bisisobutyronitrile (AIBN, 99%), and cetyltrimethylammonium bromide (CTAB, 99%) were purchased from Shanghai Chemical Reagent Co. (China). Graphite powders (99.95%) and divinylbenzene (80%) were supplied by Aladdin Chemistry Co., Ltd. Styrene and divinylbenzene were distilled under vacuum, and AIBN was recrystallized prior to use. Deionized water was used throughout the experiments.

Preparation of GO Nanosheets. GO nanosheets were prepared via a modified Hummers method[46] from graphite. The GO suspension was dialyzed in deionized water for 1 week. GO was dried in a vacuum oven at 50 °C for 24 h and was dispersed in water and sonicated (300 W) for 1 h to form the GO aqueous suspension.

Modification of GO Flakes with CTAB. In 20 mL of a GO aqueous suspension (1.0 mg mL^{-1}), 0.4, 1.0, 1.4, or 1.8 mL of CTAB solution (10.0 mg mL^{-1}) was added drop by drop with sonication. The modified GO was washed with water using a centrifugation−sonication cycle three times to remove free CTAB. CTAB-modified GO flakes were obtained after drying at 50 °C for 24 h. The GO flakes modified by various amounts of CTAB were labeled as CGO-X, where X represents the mass ratio of CTAB to GO (0.2, 0.5, 0.7, and 0.9).

Preparation of Pickering Emulsions Stabilized by CTAB-Modified GO. Pickering emulsions stabilized by CTAB-modified GO were prepared by the following method. The oil phase of the emulsions consisted of styrene and divinylbenzene in a 5:1 weight ratio. CGO-0.5, CGO-0.7, and CGO-0.9 were selected as Pickering stabilizers and dispersed into the aqueous phase. The oil phase (1.25 mL) was added to 5 mL of the modified GO suspension and shaken by hand to generate an emulsion. The GO concentration of each sample was kept at 0.8 mg mL^{-1} (according to the volume of oil phase).

Preparation of Poly-HIPEs Stabilized by CTAB-Modified GO. A typical preparation of HIPE is described as follows (samples 1−6, Table 1): an oil phase (5 mL, styrene and divinylbenzene in 5:1 mass ratio) containing 1.0 wt % of initiator AIBN was added to a 20 mL aqueous suspension of CGO-0.9. The GO concentration ranged from 0.1 to 4.0 mg mL^{-1} (relative to the oil phase). These mixtures were shaken by hand and emulsified with an FJ200-S homogenizer at 500 rpm for 5 min to form HIPEs. The Pickering HIPEs were then transferred to CentriStar Cap centrifuge tubes, and the tubes were sealed and placed in a 65 °C water bath for 24 h. The gray macroporous polymers were obtained after the products were dried in a vacuum oven at 80 °C for 24 h until a constant weight was reached.

Table 1. Concentration of Pickering Stabilizers and Pore Size of Poly-Pickering HIPEs

sample	GO concentration (mg mL^{-1})[a]	CTAB concentration (mg mL^{-1})[a]	average pore size (μm)
1	0.1	0.09	
2	0.2	0.18	352
3	0.4	0.36	227
4	0.8	0.72	148
5	2.0	1.80	67
6	4.0	3.60	40

[a]The concentration of GO and CTAB is determined according to the volume of the oil phase.

Preparation of 3D Macroporous CMGs. Macroporous polymers prepared from sample 4−6 were calcinated in a tubular furnace under a nitrogen flow at a heating rate of 10 °C min^{-1} from room temperature to 600 °C and kept at 600 °C for another 1 h. The black 3D macroporous CMGs were obtained.

Sample Characterization. Atomic force microscope (AFM) images of GO, slightly modified GO, and CGO-0.9 were obtained using a Multimode 8 in the tapping mode. The pristine GO and slightly modified GO were dispersed in water, whereas CGO-0.9 was dispersed in styrene before being tested. The samples for AFM imaging were prepared by spin coating onto freshly cleaved mica substrates.

The interlayer spacing of GO and CGO-X was determined using an X' Pert PRO (PANalytical) with Cu Kα radiation (λ = 0.154 nm). The samples were dried at 50 °C for 24 h before characterization. The XRD patterns of CMG and graphite were also recorded.

Photographs were taken by using a Canon Ixus 850IS digital camera. The type of Pickering emulsions (W/O or O/W) were assessed by the drop test.[47] The size of the initial HIPE droplets was observed by an EV5680 optical microscope after the emulsions were dropped on glass slides.

The morphologies of the macroporous polymers and CMGs were imaged using a Tescan 5136MM scanning electron microscope (SEM) and a Hitachi S-4800 field-emission scanning electron microscope (FE−SEM). All samples were placed onto carbon-coated lacy substrates. The polymer samples were sprayed with gold before observation. The void size of the poly-HIPEs was measured from the SEM images on the basis of at least 300 voids for each sample using Nano Measurer.

The Raman spectra of GO and CMG were recorded on LabRam-1B French Dilor Com with 632.8 nm laser excitation.

Nitrogen sorption isotherms were measured with a Micromeritics Tristar 3000 analyzer at 77 K. The CMGs were degassed at 200 °C under vacuum for 5 h before measurements were taken. The specific surface area of the macroporous CMGs was calculated using the Brumauer−Emmett−Teller (BET) method.

RESULTS AND DISCUSSION

Pickering HIPEs Stabilized by CTAB-Modified GO. It is well known that carboxyl, hydroxyl, and epoxy groups are introduced to GO nanosheets during the oxidation process.[46,48] The presence of these hydrophilic functional groups makes monolayer GO nanosheets disperse well in water.[49,50] The morphology of GO nanosheets was observed by AFM, as shown in Figure 1. The height of the prepared GO nanosheets is about 0.8 nm, indicating that full exfoliation is achieved. The size of the GO nanosheets ranged from 100 to 1000 nm.

It has been proven that the stability and type of Pickering emulsions are greatly affected by the wettability of solid particles.[6,47,51] Oil-in-water (O/W) emulsions are prepared using hydrophilic particles, whereas water-in-oil (W/O) emulsions can be obtained using more hydrophobic particles.[52] GO nanosheets act like surfactants at interfaces of water and oil because of their amphiphilicity.[17] The wettability of GO can be tuned by pH because the degree of ionization of the carboxyl groups is affected by pH, and O/W emulsions stabilized by GO nanosheets are obtained at lower pH values. We tried to prepare a W/O Pickering emulsion by tuning the pH of the GO suspension. However, only an O/W emulsion could be obtained because of the hydrophilicity of GO even when the

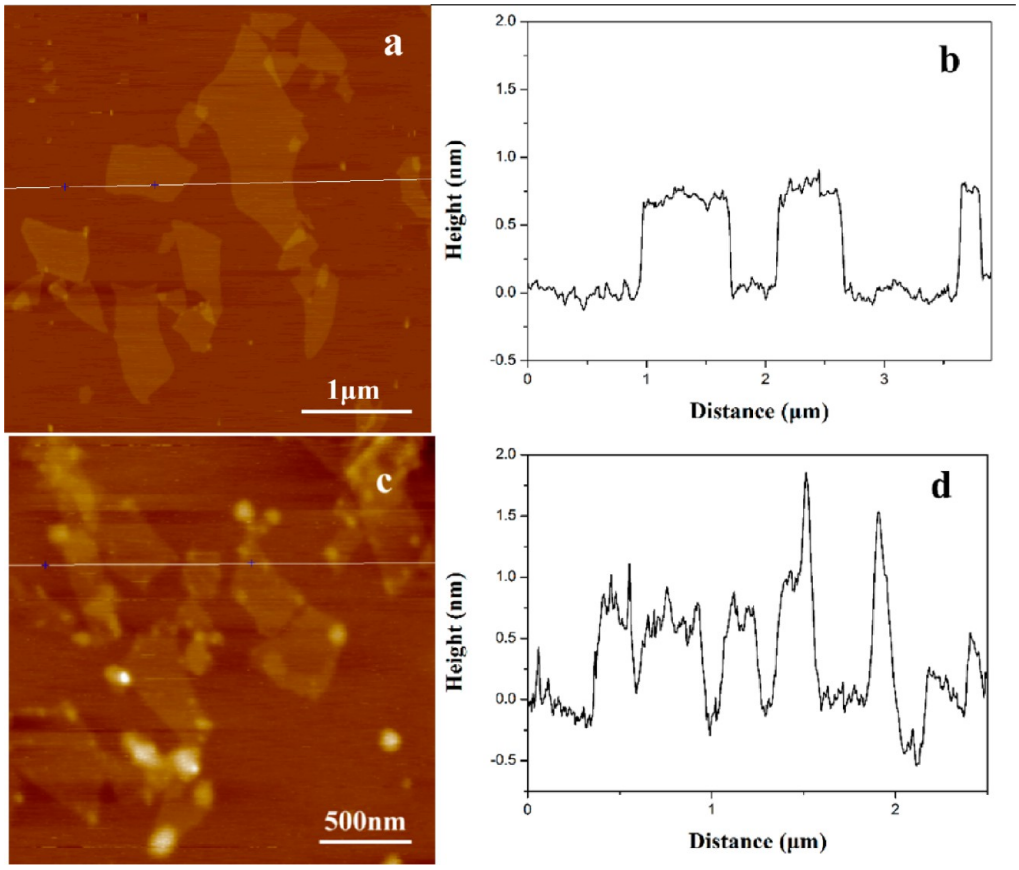

Figure 1. Tapping-mode AFM images (a, c) and height profiles (b, d) of GO (a, b) and slightly modified GO (c, d).

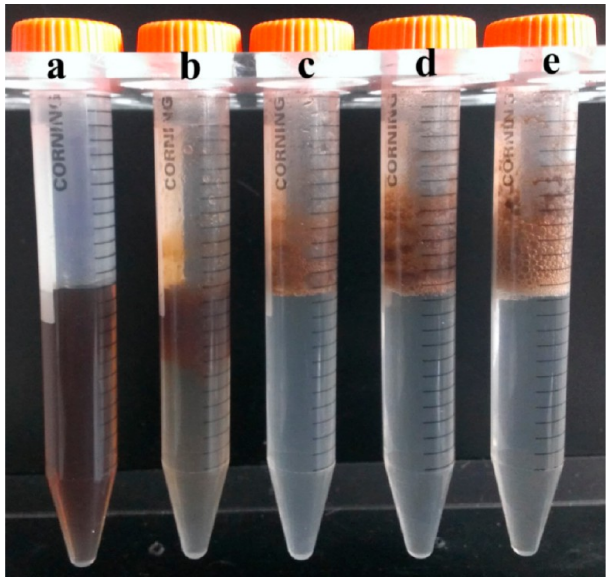

Figure 2. Photographs of aqueous dispersions of GO (a), CGO-0.2 (b), CGO-0.5 (c), CGO-0.7 (d), and CGO-0.9 (e).

aqueous phase had a high concentration (10 wt %) of HCl. Some studies have also confirmed the hydrophilic-surface nature of GO, which results in a water contact angle of GO in the range of 50−68°.[53,54]

The wettability of solid particles can be modified by surfactants. It has been proven that the phase inversion from an O/W to a W/O Pickering emulsion can take place by using

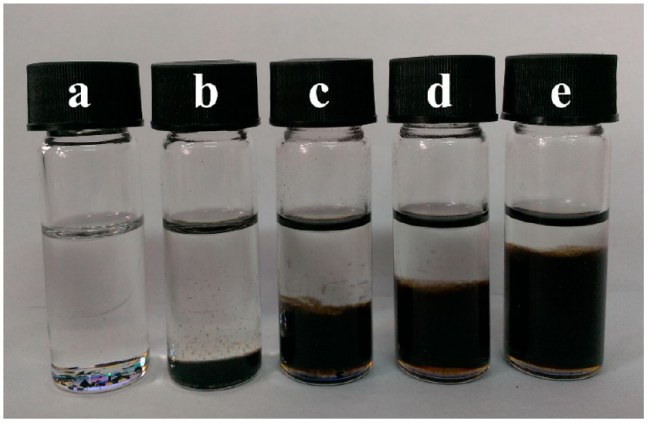

Figure 3. Photographs of dispersions of GO (a), CGO-0.2 (b), CGO-0.5 (c), CGO-0.7 (d), and CGO-0.9 (e) in styrene at a concentration of 0.5 mg mL^{-1} of GO after 1 week.

a different dosage of the surfactants.[47,51,55] Cationic surfactants are expected to be efficient to tune the surface nature of GO because of their electronegativity. Herein, CTAB is used to modify the surface property of GO nanosheets. Figure 2 shows the photographs of aqueous dispersions of pristine GO and modified GO. The pristine-GO aqueous suspension is stable and yellow-brown (Figure 2a). The obvious flocculation of GO is found after the addition of CTAB, indicating that a strong electrostatic attraction takes place. When adding a relatively small amount of CTAB (Figure 2b), GO flocculation moves to the upper layer of the aqueous phase because of the decrease of hydrophilicity. The pale-yellow aqueous phase means that there

dx.doi.org/10.1021/am4020549 | ACS Appl. Mater. Interfaces 2013, 5, 7974−7982

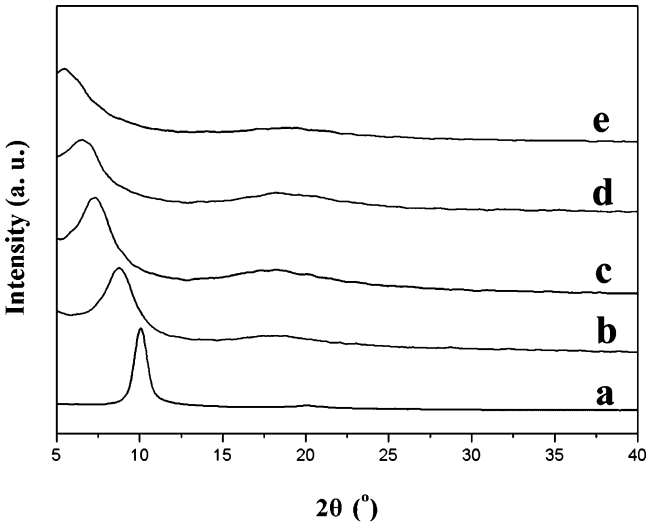

Figure 4. XRD patterns of GO (a), CGO-0.2 (b), CGO-0.5 (c), CGO-0.7 (d), and CGO-0.9 (e).

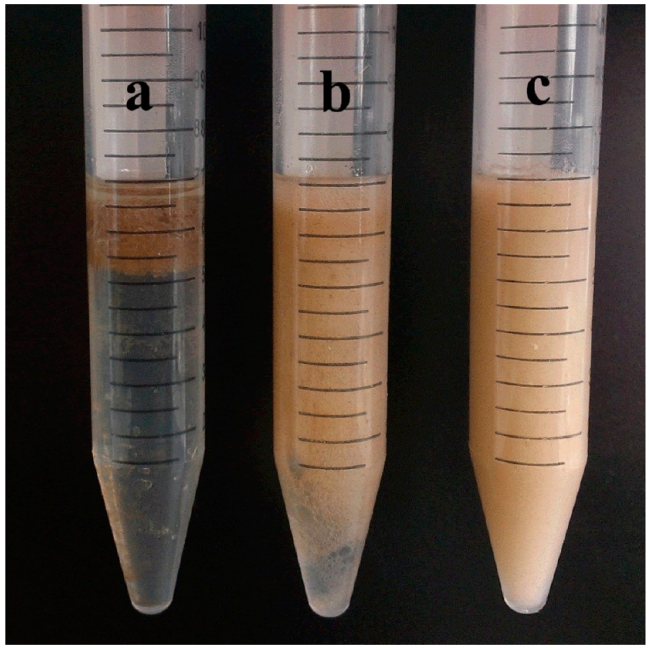

Figure 5. Photographs of Pickering emulsions stabilized by CGO-0.5 (a), CGO-0.7 (b), and CGO-0.9 (c) after 1 week.

are still some relatively hydrophilic GO. The aqueous phase becomes transparent with increased CTAB content, as shown in Figure 2c–e.

The dispersions of GO and CGO-X in styrene further illustrate the surface nature of the modified GO. In Figure 3a, it can be seen clearly that the pristine GO can be hardly dispersed in styrene resulting from the presence of plenty of polar functionalities on the surface of GO.[49] After modification, the hydrophobic alkyl chains of CTAB improve the dispersion of the GO flakes in styrene, as shown in Figure 3b–e. All of the CGO-X samples precipitate after 1 week because surfactant-modified particles usually undergo flocculation in solvents, which is helpful to stabilize Pickering emulsions.[6,56,57] The sedimentation height of modified GO became higher when more CTAB was used (Figure 3b–e). This is quite reasonable because more CTAB chains adsorbed on the surface of GO

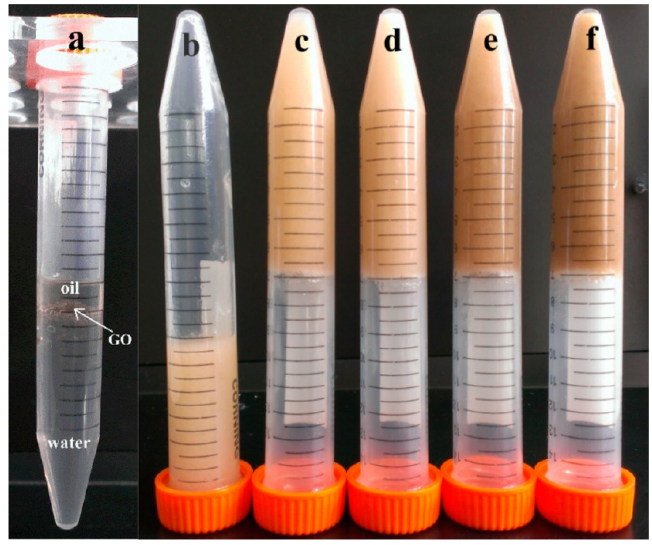

Figure 6. Photographs of samples 1–6 (a–f) after 1 week.

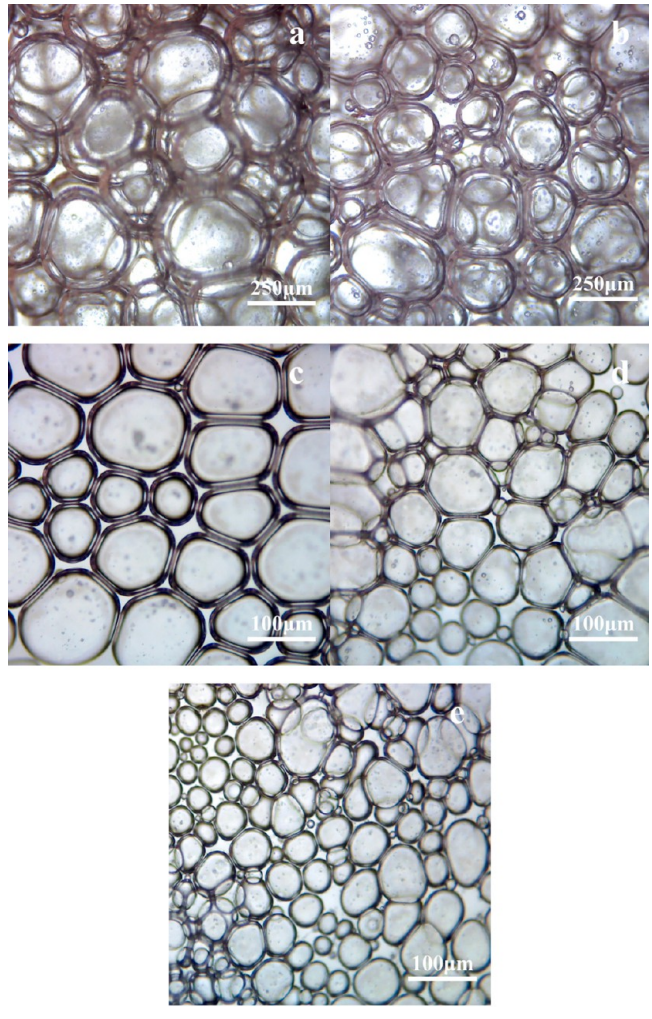

Figure 7. Optical microscopy images of Pickering HIPEs for samples 2–6 (a–e).

flakes improve their hydrophobicity and make them disperse better in nonpolar solvents to form a sedimentation with a fluffy structure.

dx.doi.org/10.1021/am4020549 | ACS Appl. Mater. Interfaces 2013, 5, 7974–7982

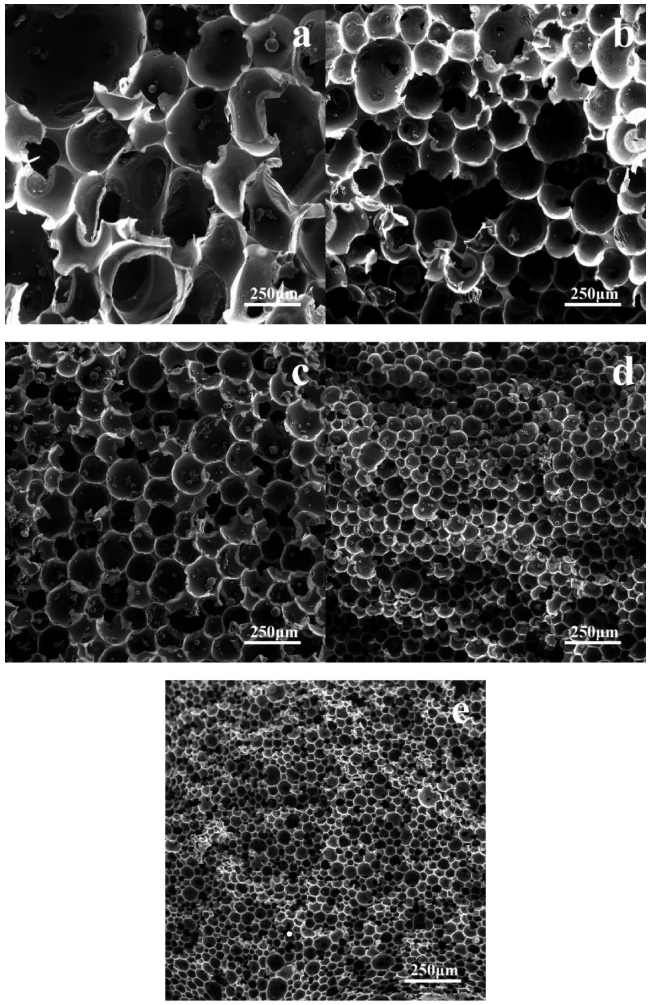

Figure 8. SEM images of poly-Pickering HIPEs for samples 2–6 (a–e).

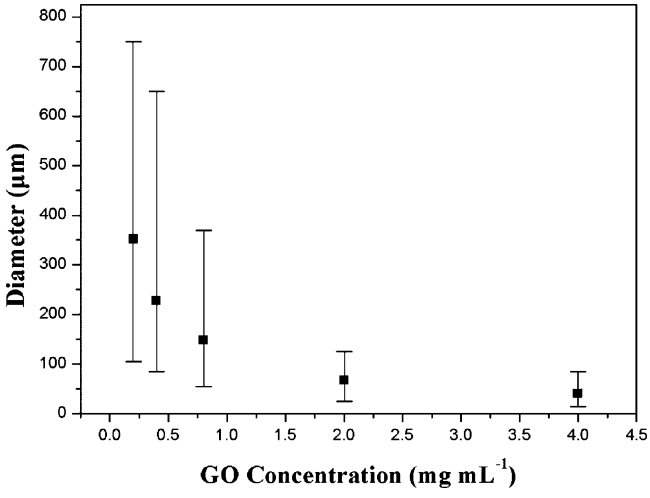

Figure 9. Void size vs GO concentration for poly-Pickering HIPEs.

The interaction between CTAB and GO is also confirmed using AFM (Figures 1 and S1). A dramatic increase in the height of CGO-0.9 is shown in Figure S1, which may be caused by the stacking of GO flakes resulting from the sufficient adsorption of CTAB molecules. The stacking of modified GO (CGO-0.2 to 0.9) makes it difficult to observe the adsorption of

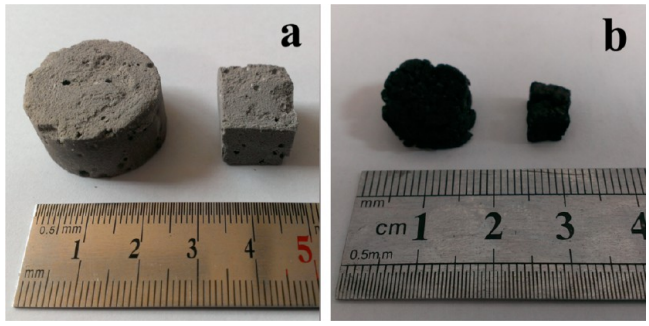

Figure 10. Photographs of macroporous polymers prepared from sample 6 (a) and the corresponding macroporous CMG monoliths after the calcination (b).

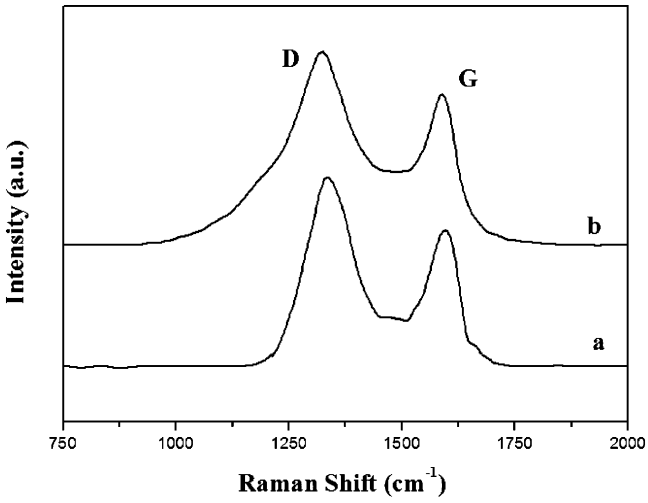

Figure 11. Raman spectra of GO (a) and CMG 3 (b).

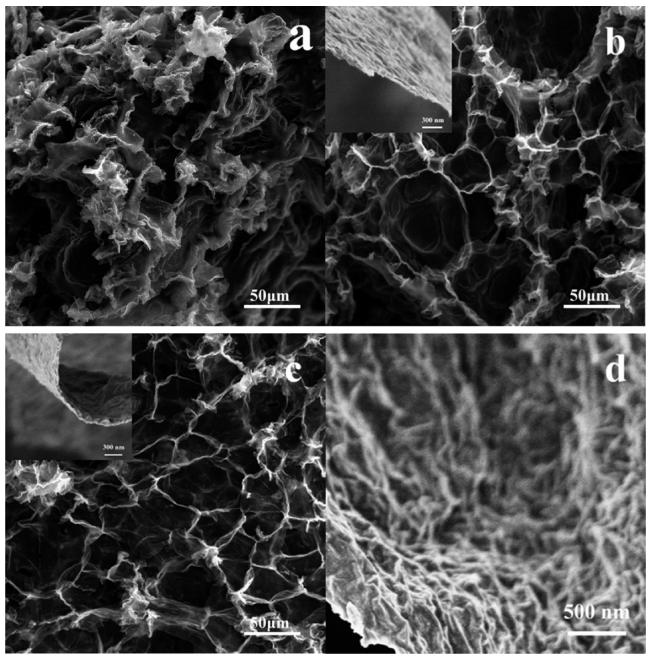

Figure 12. SEM and FE–SEM images of CMG 1 (a), 2 (b), and 3 (c, d). The insets show the pore-wall structure of each of the corresponding samples.

dx.doi.org/10.1021/am4020549 | ACS Appl. Mater. Interfaces 2013, 5, 7974–7982

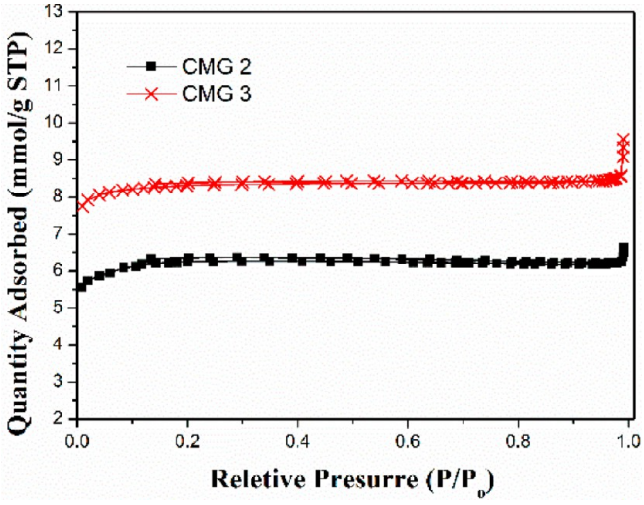

Figure 13. Nitrogen adsorption−desorption isotherms of CMG 2 (a) and 3 (b). The isotherms of CMG 3 was offset vertically by 2 mmol g^{-1} at STP.

CTAB on GO. Thus, slightly modified GO is needed for AFM characterization, and the relatively hydrophilic GO of sample CGO-0.2 in the pale-yellow aqueous phase is selected for measurement. The height of slightly modified GO ranged from 1.0 to 1.7 nm, which is higher than that of pristine GO (0.8 nm) because of the adsorption of CTAB molecules. This result is similar to the polymer-grafted graphene or graphene oxide sheets reported previously.[58−60]

XRD characterization was carried out to clarify the structure of CTAB-modified GO, as shown in Figure 4. The diffraction angle of pristine GO flakes is about 5.05°. According to the Bragg formula, the diffraction peak of GO corresponds to a layer spacing of 0.88 nm, which is in accordance with previous reports.[23,61] The diffraction angle of GO decreases gradually with the increasing content of CTAB, and the layer spacing of the GO flakes is 1.00, 1.22, 1.36, and 1.62 nm, respectively. The effective exfoliation of the GO flakes is induced by the adsorption of CTAB molecules via electrostatic attraction. In addition, the hydrocarbon chains of CTAB adsorbing on the surface improves the hydrophobicity of GO flakes dramatically, which leads to their aggregation, as shown in Figure 2. Dynamic light scattering and zeta potential measurements are the most popular methods to characterize the size and surface nature of solid particles. However, these are hard to conduct because the aqueous dispersion of CTAB-modified GO is too poor. Therefore, the attachment of CTAB on GO flakes results in the formation of an intercalated structure of GO with improved hydrophobicity, which may be suitable to stabilize W/O Pickering emulsions.

CGO-0.5, CGO-0.7, and CGO-0.9 were used to prepare Pickering HIPEs with a GO concentration of 0.8 mg mL^{-1}. The appearance of the obtained emulsions is shown in Figure 5. It is clearly seen from Figure 5a that CGO-0.5 cannot stabilize the Pickering emulsion efficiently. Plenty of water is still on the bottom, and a layer of monomer is at the top. It is confirmed that an O/W Pickering emulsion is formed on the basis of the drop test in the aqueous or oil phases, indicating the relative hydrophilicity of GO. The phase inversion of Pickering emulsions is induced by the adsorption of more CTAB molecules on the surface of GO flakes, as shown in Figure 5b. However, there is still a clear aqueous phase at the bottom. A W/O Pickering HIPE containing an 80 vol % internal phase is achieved using CGO-0.9 as the stabilizer (Figure 5c). This HIPE is quite stable for more than 1 week. Consequently, sufficient surface modification of GO nanosheets is required for the preparation of stable W/O Pickering HIPEs.

The Pickering emulsions stabilized by various amount of CGO-0.9 (Table 1) were also investigated. The photographs of the obtained Pickering emulsions are shown in Figure 6. The emulsion stabilized by a small amount of CGO-0.9 is not stable, and the two phases separate quickly. Interestingly, after phase separation, both the aqueous and oil phases are transparent and almost all CGO-0.9 locates at the oil−water interface (Figure

Scheme 1. Schematic Illustration of Poly-Pickering HIPEs and 3D Macroporous CMGs

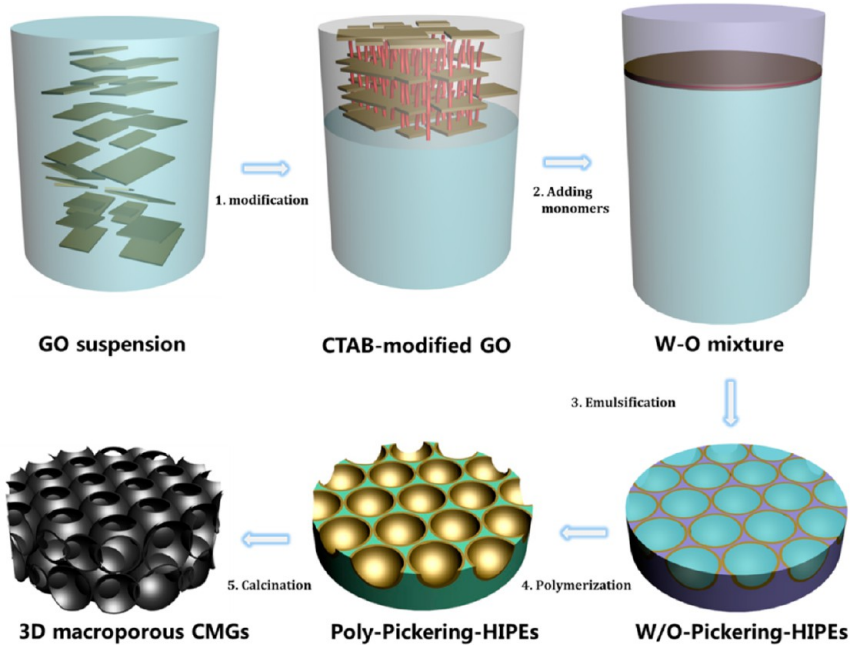

6a), indicating that the wettability of CGO-0.9 is suitable to stabilize Pickering emulsions.[6] Stable W/O Pickering HIPEs can be produced using increased concentration of CGO-0.9, as shown in Figure 6b−f. The viscosity of the Pickering HIPE is relatively low when the GO concentration is as low as 0.2 mg mL^{-1}, and the emulsion flows down when the tube is inverted. The other four samples with a higher GO concentration have an obviously high viscosity. The Pickering HIPEs with a further increased GO concentration (>8.0 mg mL^{-1}) cannot be prepared owing to the high viscosity of the emulsions, which has been found in other studies of Pickering HIPEs.[7,10,15] The droplets of each HIPE are shown in Figure 7, and an obvious decrease in size is found with the increasing concentration of CGO-0.9 because more GO flakes can stabilize the larger interfacial area similar to that of other solid particles.[17,62,63] It should be noted that CGO-0.9 is an efficient Pickering stabilizer. Only 0.2 mg mL^{-1} of GO can produce a stable W/O Pickering HIPE, which is much lower than that of other solid particles used as a Pickering stabilizer.[7,11,15]

Macroporous Polymer−Graphene Oxide Composites. After polymerization of the Pickering HIPEs, poly-Pickering HIPEs are obtained, and the morphology of the macroporous polymers is shown in Figure 8. The samples have a close-cell structure, and the sizes of the voids are consistent with the initial emulsion droplets. The average pore size of the macroporous polymers after the polymerization of samples 2−6 is listed in Table 1. Such a close-cell structure has also been found in poly-HIPEs stabilized by other kinds of solid particles.[7,11,15] There is a thin film at the point of two contacted voids. It can be seen clearly that the thin films are broken occasionally. It is quite reasonable that these films are present because Pickering emulsions are highly stable, and the solid stabilizer at the interface acts like a steric barrier against coalescence.[5] The void size of poly-Pickering HIPEs with various GO concentrations is given in Figure 9. It indicates that not only does the void size decrease but also the size distribution becomes narrow as the GO concentration increases.

3D Macroporous CMG Monoliths. As a Pickering stabilizer, GO flakes self-assemble at the interface of the oil and water phases to produce HIPEs, and after the polymerization of the HIPEs GO locates on the pore surface of the macroporous polymers. Therefore, 3D macroporous CMG monoliths are fabricated via calcination using macroporous polymers as the sacrificial templates. The CMGs prepared from sampled 4−6 were named as CMG 1−3, respectively. Figure 10 shows the appearance of the macroporous polymers and their corresponding CMGs. The gray macroporous polymers become smaller after the thermal treatment, but the shape of the monoliths is basically maintained. The black color of the final macroporous CMGs demonstrates the reduction of GO during calcination. Previous reports have also shown that most functional groups on the surface of GO fall off when heated at 230 °C with an inert gas.[64] The Raman spectra of GO and CMG obtained from sample 6 are shown in Figure 11. Two prominent peaks corresponding to D and G bands appear at about 1330 and 1580 cm^{-1}, respectively.[65] The G band is usually assigned to the E_{2g} phonon of C sp^2 atoms, whereas the D band arises from activation in the first-order scattering process of sp^3 carbons in graphene sheets.[66] The formation of defects is monitored by the intensity ratio of the D and G bands (I_D/I_G). The I_D/I_G of GO is about 1.39, and it decreases to 1.16 for CMG, suggesting the recovery of the aromatic structures and the reduction of GO after calcination.

The SEM and FE−SEM images (Figure 12) reveal the macroporous structure of the obtained CMGs. All of these samples were not sprayed with gold before observation because of the intrinsic electrically conductive nature of CMGs. It is clearly seen that the pore structure of CMG 1 is almost destroyed after calcination, whereas the other two samples with increased GO concentration well preserve their macroporous structure. This means that the lower content of GO flakes is insufficient to support the pore structure during calcination even if macroporous polymers can be produced. The macropores of porous polymers obtained from samples 5 and 6 are deformed after the thermal treatment, as shown in Figures 8 and 12, which is consistent with the apparent volume shrinkage. The wrinkled morphology of the macropore surface of CMG 3 can be seen in Figure 12d. The insets of the FE−SEM images (Figure 12b,c) demonstrate that the pore-wall thickness of CMGs ranges from 10 to 50 nm.

The N_2 adsorption−desorption plots of CMG 2 and 3 are both similar to a type I isotherm[67] with steep adsorptions at a relative pressure of $P/P_0 < 0.02$, suggesting micropores in the CMGs. The adsorption of CTAB on the surface of GO flakes has been confirmed by the AFM images (Figure 1) and XRD patterns (Figure 4), which reveal the intercalated structure of the CTAB-modified GO. During calcination, the CTAB chains adsorbed on the surface of the GO flakes are decomposed, and micropores are formed in macroporous CMGs. The microporous structure of two CMG samples is similar because of the same modification of GO with CTAB. It is reasonable that these macroporous CMGs have a close specific surface area (487 and 491 $m^2\ g^{-1}$ for CMG 2 and 3, respectively) because micropores may make a major contribution to the specific surface area of the macroporous samples. In addition, the hysteresis loops are small, suggesting few mesopores in CMGs, and an obvious upturn of P/P_0 close to 1.0 is an indication of macropores.[67,68] As shown in Figure S2, the similar pore-size distribution of CMG 2 and 3 is also clearly seen.

The XRD pattern (Figure S3) demonstrates the amorphous structure of CMG, indicating that a layered structure like graphite cannot be formed after removing the polymer substrate and CTAB adsorbed on the surface of GO. The tight stacking of CMG flakes may be hindered by the microporous structure in CMGs, which is proven by the nitrogen adsorption−desorption isotherms.

According to these results, we propose a facile strategy (Scheme 1) to prepare macroporous polymer−GO composites and 3D CMGs. The pristine GO nanosheets are relatively hydrophilic, and their hydrophobicity is improved by the adsorption of CTAB resulting from electrostatic interactions. Stable W/O HIPEs are obtained using surface-modified GO as a Pickering stabilizer. After the polymerization, macroporous polymer−GO composites with a close-cell structure are prepared, and their pore size is determined by GO concentration. Three-dimensional macroporous CMG monoliths with a high surface area are fabricated using porous polymers as the sacrificial templates.

CONCLUSIONS

We have demonstrated a novel approach to prepare macroporous polymer−GO composites via W/O Pickering HIPE templates. The hydrophobicity of GO flakes is greatly improved by the adsorption of CTAB, and a stable Pickering HIPE can be

produced using CTAB-modified GO even at a low concentration (0.2 mg mL^{-1}). The poly-Pickering HIPEs have a close-cell structure, and some open windows between the two voids are also found. The modified GO with a higher concentration used to stabilize HIPEs leads to the macroporous polymers having a smaller void size and a narrower size distribution. Three-dimensional macroporous CMG monoliths with a large specific surface area of up to 490 m^2 g^{-1} are successfully fabricated after removing the porous polymer substrates. The microporous structure of CMGs may be induced by the decomposition of CTAB molecules adsorbed on the GO's surface.

■ ASSOCIATED CONTENT

Supporting Information

Tapping-mode AFM image and height profile of CGO-0.9, pore size distributions for CMG 2 and 3, and XRD patterns of pristine graphite and CMG 3. This material is available free of charge via the Internet at http://pubs.acs.org.

■ AUTHOR INFORMATION

Corresponding Author

*E-mail: wanght@fudan.edu.cn. Tel: +86-21-6564-2392. Fax: +86-21-6564-0293.

Notes

The authors declare no competing financial interest.

■ REFERENCES

(1) Cameron, N. R. *Polymer* **2005**, *46*, 1439−1449.
(2) Williams, J. M. *Langmuir* **1991**, *7*, 1370−1377.
(3) Williams, J. M.; Gray, A. J.; Wilkerson, M. H. *Langmuir* **1990**, *6*, 437−444.
(4) Cameron, N. R.; Barbetta, A. *J. Mater. Chem.* **2000**, *10*, 2466−2471.
(5) Colver, P. J.; Bon, S. A. F. *Chem. Mater.* **2007**, *19*, 1537−1539.
(6) Binks, B. P. *Curr. Opin. Colloid Interface Sci.* **2002**, *7*, 21−41.
(7) Ikem, V. O.; Menner, A.; Bismarck, A. *Angew. Chem., Int. Ed.* **2008**, *47*, 8277−8279.
(8) Viswanathan, P.; Chirasatitsin, S.; Ngamkham, K.; Engler, A. J.; Battaglia, G. *J. Am. Chem. Soc.* **2012**, *134*, 20103−20109.
(9) Haibach, K.; Menner, A.; Powell, R.; Bismarck, A. *Polymer* **2006**, *47*, 4513−4519.
(10) Hermant, M. C.; Klumperman, B.; Koning, C. E. *Chem. Commun.* **2009**, 2738−2740.
(11) Vilchez, A.; Rodriguez-Abreu, C.; Esquena, J.; Menner, A.; Bismarck, A. *Langmuir* **2011**, *27*, 13342−13352.
(12) Zhang, S.; Chen, J. *Chem. Commun.* **2009**, 2217−2219.
(13) Zhang, S.; Zhu, Y.; Hua, Y.; Jegat, C.; Chen, J.; Taha, M. *Polymer* **2011**, *52*, 4881−4890.
(14) Zou, S.; Wang, C.; Wei, Z.; Liu, H.; Tong, Z. *Acta Chim. Sin.* **2012**, *70*, 133−136.
(15) Ikem, V. O.; Menner, A.; Bismarck, A. *Langmuir* **2010**, *26*, 8836−8841.
(16) Menner, A.; Verdejo, R.; Shaffer, M.; Bismarck, A. *Langmuir* **2007**, *23*, 2398−2403.
(17) Kim, J.; Cote, L. J.; Kim, F.; Yuan, W.; Shull, K. R.; Huang, J. X. *J. Am. Chem. Soc.* **2010**, *132*, 8180−8186.
(18) Guo, P.; Song, H.; Chen, X. *J. Mater. Chem.* **2010**, *20*, 4867−4874.
(19) Song, X. H.; Yang, Y. F.; Liu, J. C.; Zhao, H. Y. *Langmuir* **2011**, *27*, 1186−1191.
(20) Gudarzi, M. M.; Sharif, F. *Soft Matter* **2011**, *7*, 3432−3440.
(21) Yin, G. N.; Zheng, Z.; Wang, H. T.; Du, Q. G.; Zhang, H. D. *J. Colloid Interface Sci.* **2013**, *394*, 192−198.
(22) Dreyer, D. R.; Park, S.; Bielawski, C. W.; Ruoff, R. S. *Chem. Soc. Rev.* **2010**, *39*, 228−240.
(23) Fang, M.; Wang, K.; Lu, H.; Yang, Y.; Nutt, S. *J. Mater. Chem.* **2009**, *19*, 7098−7105.
(24) Li, D.; Muller, M. B.; Gilje, S.; Kaner, R. B.; Wallace, G. G. *Nat. Nanotechnol.* **2008**, *3*, 101−105.
(25) Rao, C. N. R.; Sood, A. K.; Subrahmanyam, K. S.; Govindaraj, A. *Angew. Chem., Int. Ed.* **2009**, *48*, 7752−7777.
(26) Geim, A. K.; Novoselov, K. S. *Nat. Mater.* **2007**, *6*, 183−191.
(27) Seger, B.; Kamat, P. V. *J. Phys. Chem. C* **2009**, *113*, 7990−7995.
(28) Yan, X.; Chen, J.; Yang, J.; Xue, Q.; Miele, P. *ACS Appl. Mater. Interfaces* **2010**, *2*, 2521−2529.
(29) Yoo, E.; Kim, J.; Hosono, E.; Zhou, H.; Kudo, T.; Honma, I. *Nano Lett.* **2008**, *8*, 2277−2282.
(30) Jianhua, L.; Junwei, A.; Yecheng, Z.; Yuxiao, M.; Mengliu, L.; Mei, Y.; Songmei, L. *ACS Appl. Mater. Interfaces* **2012**, *4*, 2870−2876.
(31) Huang, X.; Qi, X.; Boey, F.; Zhang, H. *Chem. Soc. Rev.* **2012**, *41*, 666−686.
(32) Sun, Y.; Wu, Q.; Shi, G. *Energy Environ. Sci.* **2011**, *4*, 1113−1132.
(33) Stoller, M. D.; Park, S.; Zhu, Y.; An, J.; Ruoff, R. S. *Nano Lett.* **2008**, *8*, 3498−3502.
(34) Qiu, H.; Dong, X.; Sana, B.; Peng, T.; Paramelle, D.; Chen, P.; Lim, S. *ACS Appl. Mater. Interfaces* **2013**, *5*, 782−787.
(35) Yin, S.; Niu, Z.; Chen, X. *Small* **2012**, *8*, 2458−2463.
(36) Li, C.; Shi, G. *Nanoscale* **2012**, *4*, 5549−5563.
(37) Vickery, J. L.; Patil, A. J.; Mann, S. *Adv. Mater.* **2009**, *21*, 2180−2184.
(38) Dong, X.; Wang, X.; Wang, L.; Song, H.; Zhang, H.; Huang, W.; Chen, P. *ACS Appl. Mater. Interfaces* **2012**, *4*, 3129−3133.
(39) Bai, H.; Li, C.; Wang, X.; Shi, G. *J. Phys. Chem. C* **2011**, *115*, 5545−5551.
(40) Lee, S. H.; Kim, H. W.; Hwang, J. O.; Lee, W. J.; Kwon, J.; Bielawski, C. W.; Ruoff, R. S.; Kim, S. O. *Angew. Chem., Int. Ed.* **2010**, *49*, 10084−10088.
(41) Korkut, S.; Roy-Mayhew, J. D.; Dabbs, D. M.; Milius, D. L.; Aksay, I. A. *ACS Nano* **2011**, *5*, 5214−5222.
(42) Dikin, D. A.; Stankovich, S.; Zimney, E. J.; Piner, R. D.; Dommett, G. H. B.; Evmenenko, G.; Nguyen, S. T.; Ruoff, R. S. *Nature* **2007**, *448*, 457−460.
(43) Choi, B. G.; Yang, M.; Hong, W. H.; Choi, J. W.; Huh, Y. S. *ACS Nano* **2012**, *6*, 4020−4028.
(44) Huang, X.; Qian, K.; Yang, J.; Zhang, J.; Li, L.; Yu, C.; Zhao, D. *Adv. Mater.* **2012**, *24*, 4419−4423.
(45) Fan, D.; Liu, Y.; He, J.; Zhou, Y.; Yang, Y. *J. Mater. Chem.* **2012**, *22*, 1396−1402.
(46) Hummers, W. S.; Offeman, R. E. *J. Am. Chem. Soc.* **1958**, *80*, 1339−1339.
(47) Binks, B. P.; Lumsdon, S. O. *Langmuir* **2000**, *16*, 8622−8631.
(48) Titelman, G. I.; Gelman, V.; Bron, S.; Khalfin, R. L.; Cohen, Y.; Bianco-Peled, H. *Carbon* **2005**, *43*, 641−649.
(49) Paredes, J. I.; Villar-Rodil, S.; Martinez-Alonso, A.; Tascon, J. M. D. *Langmuir* **2008**, *24*, 10560−10564.
(50) Lin, Z.; Liu, Y.; Wong, C. P. *Langmuir* **2010**, *26*, 16110−16114.
(51) Wang, J.; Yang, F.; Li, C. F.; Liu, S. Y.; Sun, D. J. *Langmuir* **2008**, *24*, 10054−10061.
(52) Aveyard, R.; Binks, B. P.; Clint, J. H. *Adv. Colloid Interface Sci.* **2003**, *100−102*, 503−546.
(53) Moon, I. K.; Lee, J.; Ruoff, R. S.; Lee, H. *Nat. Commun.* **2010**, *1*, 73-1−73-6.
(54) Wang, S. R.; Zhang, Y.; Abidi, N.; Cabrales, L. *Langmuir* **2009**, *25*, 11078−11081.
(55) Lan, Q.; Yang, F.; Zhang, S. Y.; Liu, S. Y.; Xu, H.; Sun, D. J. *Colloids Surf., A* **2007**, *302*, 126−135.
(56) Zhao, Y.; Wang, H.; Song, X.; Du, Q. *Macromol. Chem. Phys.* **2010**, *211*, 2517−2529.
(57) Hu, H.; Wang, H.; Du, Q. *Soft Matter* **2012**, *8*, 6816−6822.
(58) Deng, Y.; Li, Y.; Dai, J.; Lang, M.; Huang, X. *J. Polym. Sci., Part A-1* **2011**, *49*, 1582−1590.
(59) Deng, Y.; Li, Y.; Dai, J.; Lang, M.; Huang, X. *J. Polym. Sci., Part A-1* **2011**, *49*, 4747−4755.

(60) Deng, Y.; Zhang, J. Z.; Li, Y.; Hu, J.; Yang, D.; Huang, X. *J. Polym. Sci., Part A-1* **2012**, *50*, 4451−4458.
(61) Zhu, C.; Guo, S.; Fang, Y.; Dong, S. *ACS Nano* **2010**, *4*, 2429−2437.
(62) Ashby, N. P.; Binks, B. P. *Phys. Chem. Chem. Phys.* **2000**, *2*, 5640−5646.
(63) Binks, B. P.; Fletcher, P. D. I.; Holt, B. L.; Parker, J.; Beaussoubre, P.; Wong, K. *Phys. Chem. Chem. Phys.* **2010**, *12*, 11967−11974.
(64) McAllister, M. J.; Li, J. L.; Adamson, D. H.; Schniepp, H. C.; Abdala, A. A.; Liu, J.; Herrera-Alonso, M.; Milius, D. L.; Car, R.; Prud'homme, R. K.; Aksay, I. A. *Chem. Mater.* **2007**, *19*, 4396−4404.
(65) Kudin, K. N.; Ozbas, B.; Schniepp, H. C.; Prud'homme, R. K.; Aksay, I. A.; Car, R. *Nano Lett.* **2008**, *8*, 36−41.
(66) Zhou, Y.; Bao, Q.; Tang, L. A. L.; Zhong, Y.; Loh, K. P. *Chem. Mater.* **2009**, *21*, 2950−2956.
(67) Sing, K. S. W.; Everett, D. H.; Haul, R. A. W.; Moscou, L.; Pierotti, R. A.; Rouquerol, J.; Siemieniewska, T. *Pure Appl. Chem.* **1985**, *57*, 603−619.
(68) Ungureanu, S.; Laurent, G.; Deleuze, H.; Babot, O.; Achard, M. F.; Popa, M. I.; Sanchez, C.; Backov, R. *Colloids Surf., A* **2010**, *360*, 85−93.